nature human behaviour

ARTICLES

https://doi.org/10.1038/s41562-021-01161-1

Check for updates

Brain stimulation and brain lesions converge on common causal circuits in neuropsychiatric disease

Shan H. Siddiqi[1,2]✉, Frederic L. W. V. J. Schaper[1,3,4], Andreas Horn[1,3,5], Joey Hsu[6], Jaya L. Padmanabhan[1], Amy Brodtmann[7], Robin F. H. Cash[7,8], Maurizio Corbetta[9,10], Ki Sueng Choi[11], Darin D. Dougherty[2,12], Natalia Egorova[13,14], Paul B. Fitzgerald[15], Mark S. George[16,17], Sophia A. Gozzi[18], Frederike Irmen[19], Andrea A. Kuhn[5], Kevin A. Johnson[20], Andrew M. Naidech[21], Alvaro Pascual-Leone[3,22,23], Thanh G. Phan[18], Rob P. W. Rouhl[4,24,25], Stephan F. Taylor[26], Joel L. Voss[21], Andrew Zalesky[7,8], Jordan H. Grafman[21,27], Helen S. Mayberg[11] and Michael D. Fox[1,3]

Damage to specific brain circuits can cause specific neuropsychiatric symptoms. Therapeutic stimulation to these same circuits may modulate these symptoms. To determine whether these circuits converge, we studied depression severity after brain lesions ($n = 461$, five datasets), transcranial magnetic stimulation ($n = 151$, four datasets) and deep brain stimulation ($n = 101$, five datasets). Lesions and stimulation sites most associated with depression severity were connected to a similar brain circuit across all 14 datasets ($P < 0.001$). Circuits derived from lesions, deep brain stimulation and transcranial magnetic stimulation were similar ($P < 0.0005$), as were circuits derived from patients with major depression versus other diagnoses ($P < 0.001$). Connectivity to this circuit predicted out-of-sample antidepressant efficacy of transcranial magnetic stimulation and deep brain stimulation sites ($P < 0.0001$). In an independent analysis, 29 lesions and 95 stimulation sites converged on a distinct circuit for motor symptoms of Parkinson's disease ($P < 0.05$). We conclude that lesions, transcranial magnetic stimulation and DBS converge on common brain circuitry that may represent improved neurostimulation targets for depression and other disorders.

Causal neuroanatomy can be mapped in animal models by precisely modulating different brain circuits in well-controlled experiments[1,2]. However, it can be challenging to translate these findings into human therapeutics[3,4]. In humans, mapping of psychiatric symptoms is based primarily on correlation, resulting in a 'causality' gap when attempting to translate this information into effective treatments. Causality may be inferred in humans based on the clinical effects of focal brain lesions, transcranial magnetic stimulation (TMS) and deep brain stimulation (DBS)[2]. These modalities have each been used to link depression symptoms to specific brain circuits based on the location of lesions or stimulation sites that affect depression severity[2,5–9]. Each result has been proposed as a potential solution to the causality gap between neuroimaging correlates and effective treatments[2,10].

It remains unclear whether these three causal sources of information converge on the same circuit or therapeutic target[2,11,12]. Heterogeneity in lesion location, stimulation site location, neuromodulation modality, patient population, depression symptoms, depression subtypes and numerous other factors argue against a common neuroanatomical substrate. If these causal sources of

[1]Center for Brain Circuit Therapeutics, Brigham and Women's Hospital, Boston, MA, USA. [2]Department of Psychiatry, Harvard Medical School, Boston, MA, USA. [3]Department of Neurology, Harvard Medical School, Boston, MA, USA. [4]Department of Neurology, Maastricht University Medical Center, Maastricht, the Netherlands. [5]Movement Disorders and Neuromodulation Unit, Department for Neurology, Charité University Medicine Berlin, Berlin, Germany. [6]University of Pittsburgh School of Medicine, Pittsburgh, PA, USA. [7]Melbourne Neuropsychiatry Centre, The University of Melbourne, Melbourne, Victoria, Australia. [8]Department of Biomedical Engineering, The University of Melbourne, Melbourne, Victoria, Australia. [9]Department of Neuroscience, Padova Neuroscience Center (PNC), Venetian Institute of Molecular Medicine (VIMM), University of Padova, Padova, Italy. [10]Departments of Neurology, Radiology, Bioengineering, and Neuroscience, Washington University, St. Louis, MO, USA. [11]Nash Family Center for Advanced Circuit Therapeutics, Icahn School of Medicine at Mount Sinai, New York, NY, USA. [12]Department of Psychiatry, Massachusetts General Hospital, Boston, MA, USA. [13]Melbourne School of Psychological Sciences, University of Melbourne, Melbourne, Victoria, Australia. [14]The Florey Institute of Neuroscience and Mental Health, Melbourne, Victoria, Australia. [15]Epworth Centre for Innovation in Mental Health, Epworth Healthcare and Monash University Department of Psychiatry, Camberwell, Victoria, Australia. [16]Brain Stimulation Laboratory, Psychiatry Department, Medical University of South Carolina, Charleston, SC, USA. [17]Ralph H. Johnson VA Medical Center, Charleston, SC, USA. [18]Department of Neurology, Monash Health and Department of Medicine, School of Clinical Sciences, Monash University, Clayton, Victoria, Australia. [19]Department of Neurology, Charité – Universitätsmedizin Berlin, corporate member of Freie Universität Berlin, Humboldt-Universität zu Berlin and Berlin Institute of Health, Berlin, Germany. [20]School of Medicine, Florida State University, Tallahassee, FL, USA. [21]Feinberg School of Medicine, Northwestern University, Chicago, IL, USA. [22]Hinda and Arthur Marcus Institute for Aging Research and Center for Memory Health, Hebrew SeniorLife, Boston, MA, USA. [23]Guttmann Brain Health Institut, Universitat Autonoma, Barcelona, Spain. [24]School for Mental Health and Neuroscience, Maastricht University, Maastricht, the Netherlands. [25]Academic Center for Epileptology Kempenhaeghe/Maastricht University Medical Center, Maastricht, the Netherlands. [26]Department of Psychiatry, University of Michigan School of Medicine, Ann Arbor, MI, USA. [27]Shirley Ryan AbilityLab, Chicago, IL, USA. ✉e-mail: shsiddiqi@bwh.harvard.edu

information converge on a similar brain circuit despite this heterogeneity, this would have implications for localization and treatment of depression and for bridging the causality gap more generally[2]. For example, it has been proposed that TMS and DBS sites connected to similar circuits may modulate similar symptoms[13], lesions causing a symptom may be connected to the same circuit as brain stimulation targets that relieve that symptom[5] and similar symptoms map to similar circuits across different diagnoses[6,14]. Confirmation of these hypotheses may lead to a transformative framework for targeting brain stimulation treatments[2,12].

To address these questions, we analysed 14 independent datasets of patients with brain lesions, TMS or DBS. Each dataset included variability in the lesion or stimulation locations and variability in depression symptoms, measured after the lesion or before and after therapeutic brain stimulation. We also extended this approach to three additional datasets of patients with brain lesions or DBS sites associated with motor symptoms of Parkinson's disease (PD). The brain regions functionally connected to each location were identified using a normative connectome database. This method identifies a polysynaptic brain circuit underlying each location, allowing one to test whether lesions or stimulation sites in different brain regions intersect the same population-derived circuit[5]. We test whether TMS and DBS sites that affect depression are connected to the same brain circuit, whether lesion locations associated with depression and stimulation sites that affect depression are connected to the same brain circuit, whether this circuit is associated with depression severity irrespective of baseline diagnosis and whether this approach is relevant beyond depression.

Results

Characteristics of included datasets. We identified 14 datasets including 461 lesions (Fig. 1a)[15], 151 TMS sites (Fig. 1b)[8,16–18] and 101 DBS sites (Fig. 1c)[9,19–23] (Supplementary Table 1). Five datasets included patients who were evaluated for depression severity after penetrating brain injury, ischaemic stroke or haemorrhagic stroke. Seven datasets included patients who were treated for primary major depressive disorder (MDD) with either TMS (four datasets) or DBS (three datasets). Finally, two datasets included patients receiving DBS for other disorders (PD or epilepsy), but which measured change in depressive symptoms as a potential side effect.

Similar 'depression circuits' across 14 independent datasets. The location of each lesion or brain stimulation site (Fig. 2a–c, top panels) was mapped to an underlying brain circuit using a large normative connectome database ($n=1{,}000$) and previously validated methods (Fig. 2a–c, bottom panels)[5]. The normative connectome was used to estimate connectivity of each lesion or stimulation site to every voxel in the brain. At each voxel, a Pearson r value was computed for the correlation between depression score and lesion or stimulation site connectivity to that voxel (Fig. 2a–c, right panels), yielding a population-derived 'circuit map' for each of the 14 datasets (Supplementary Fig. 1).

Cross-dataset similarity was assessed by computing the spatial correlation between each pair of circuit maps (for example, dataset 1 versus dataset 2) and by comparing each circuit map with a combined map from the other 13 datasets. Significance was assessed using permutation testing, in which the spatial correlation was re-computed after randomly pairing each patient's lesion or stimulation site with a different patient's depression score within the same dataset[6]. The average pairwise similarity between circuit maps, weighted by sample size, was higher than expected by chance (mean spatial $r=0.24$, 95% CI 0.19 to 0.29, $P<0.001$) (Fig. 3a and Supplementary Fig. S2a) and similar to a weighted mean map generated from the other 13 datasets (mean spatial $r=0.45$, 95% CI 0.33 to 0.57, $P<0.001$). Results were unchanged when using Kendall tau ($P<0.001$) or Euclidean distance ($P=0.0013$) instead of Pearson correlation or when including lesion size as a covariate.

To rule out methodological bias, we conducted a control analysis using patient age instead of depression scores. Age is presumably unrelated to stimulation or lesion location, so we hypothesized that this analysis would yield significantly weaker cross-dataset similarity. Indeed, the 14 control maps did not match one another (mean spatial $r=-0.02$, 95% CI −0.09 to 0.05, $P=0.86$, Bayes factor $(BF)_{01}=1.01$) and did not match a map generated from the other 13 datasets (mean spatial $r=-0.01$, 95% CI −0.14 to 0.11, $BF_{01}=1.001$). The control maps did not match the depression circuit maps (mean spatial $r=-0.05$, 95% CI −0.12 to 0.02, $P=0.93$, $BF_{01}=1.003$). Similarity between control maps was significantly weaker than similarity between depression circuit maps ($P=0.0023$).

Convergence across brain lesions, TMS and DBS. To determine whether lesions, TMS and DBS converge on the same circuit, we grouped the different datasets according to modality. Depression circuit maps derived from brain lesion datasets were similar to circuit maps derived from TMS datasets (mean spatial $r=0.28$, 95% CI 0.17 to 0.39, $P=0.0025$), DBS datasets (mean spatial $r=0.19$, 95% CI 0.10 to 0.28, $P=0.0037$) or both neuromodulation modalities combined (mean spatial $r=0.25$, 95% CI 0.18 to 0.32, $P<0.001$) (Fig. 3 and Supplementary Fig. 2a). Depression circuit maps derived from TMS were similar to those derived from DBS (mean spatial $r=0.25$, 95% CI 0.11 to 0.39, $P<0.001$) (Fig. 3 and Supplementary Fig. 2a).

As a control, this analysis was also repeated using patient age instead of depression score. We hypothesized that this analysis would yield significantly weaker cross-dataset spatial correlation. Age-based circuit maps derived from brain lesions were not similar to those derived from TMS (mean spatial $r=-0.04$, 95% CI −0.17 to 0.09, $P=0.70$, $BF_{01}=1.07$), DBS (mean spatial $r=-0.14$, 95% CI −0.26 to −0.02, $P=0.97$, $BF_{01}=6.8$) or both neuromodulation modalities combined (mean spatial $r=-0.07$, 95% CI −0.17 to 0.02, $BF_{01}=3.4$). Control maps derived from TMS were not similar to those derived from DBS (mean spatial $r=0.01$, 95% CI −0.14 to 0.16, $P=0.43$, $BF_{01}=0.99$). In all cases, similarity between control maps was significantly weaker than similarity between depression circuit maps ($P=0.0038$). Control maps from neuromodulation datasets did not match depression circuit maps from lesion datasets (mean spatial $r=-0.11$, 95% CI −0.19 to −0.03, $BF_{01}=16.9$). Control maps from lesion datasets also did not significantly match depression circuit maps from neuromodulation datasets (mean spatial $r=0.07$, 95% CI −0.02 to 0.17), although Bayesian analysis indicates moderate evidence for a correlation ($BF_{01}=0.29$) (Fig. 4a).

Finally, we assessed whether within-modality similarity of our depression circuit maps was stronger than between-modality similarity. We compared each depression circuit map with a combined map generated from the remaining datasets within a modality (for example, TMS dataset 1 versus three other TMS datasets) or between different modalities (for example, TMS dataset 1 versus nine DBS/lesion datasets). Within-modality similarity (spatial $r=0.46$) was identical to between-modality similarity (spatial $r=0.46$). We also repeated this analysis using pairwise comparisons between circuit maps, which yielded a similar result (spatial $r=0.24$ versus $r=0.25$, respectively).

The circuit is transdiagnostic but specific to depression. We compared depression circuit maps derived from datasets of patients with MDD (seven datasets, $n=199$) with those derived from datasets of patients with other diagnoses such as stroke, penetrating head trauma, PD and epilepsy (seven datasets, $n=518$). Depression circuit maps derived from MDD datasets were similar to depression circuit maps derived from patients without MDD

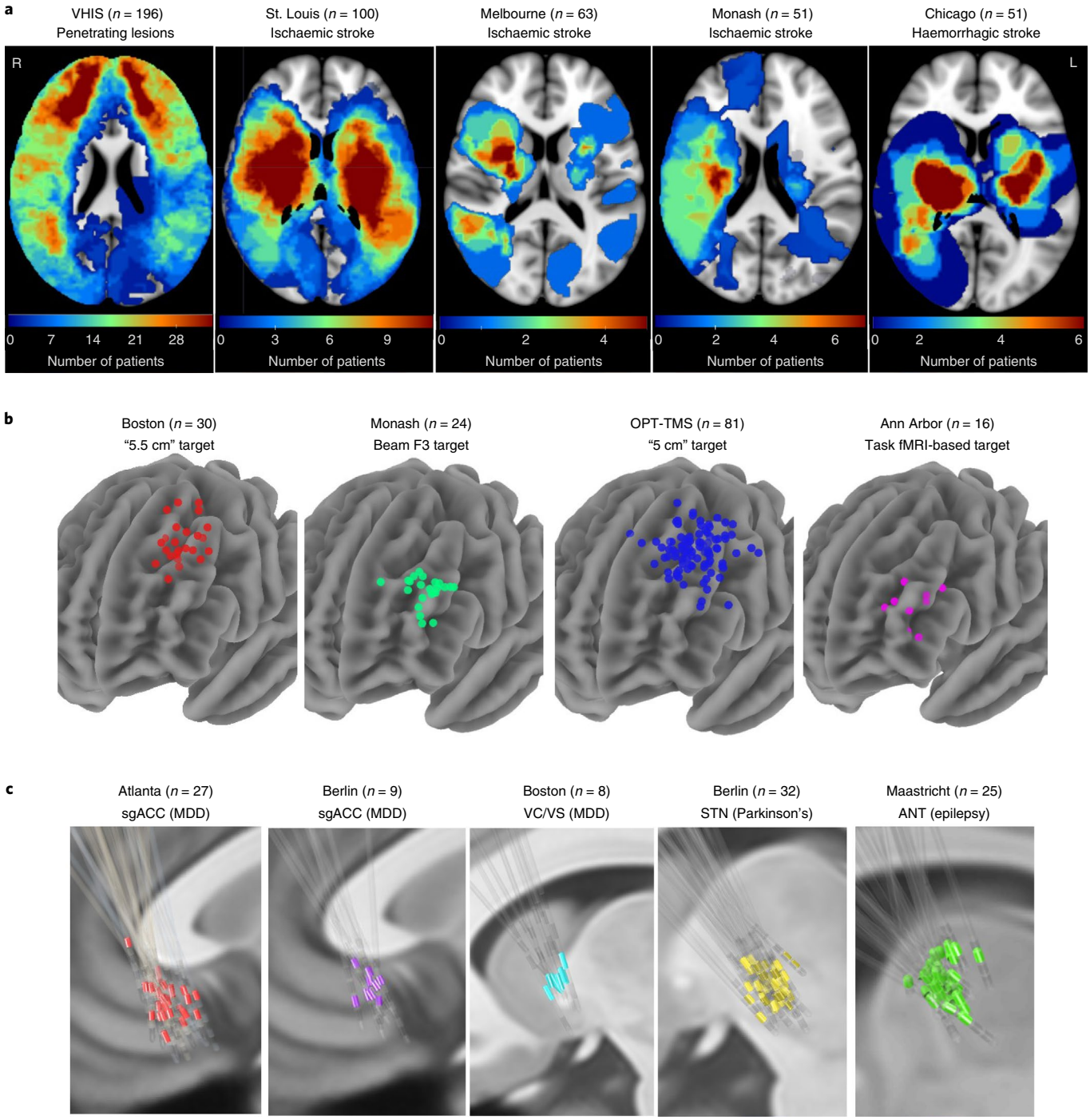

Fig. 1 | Lesion locations and brain stimulation sites across 14 datasets. a–**c**, The analysis included 461 brain lesions across five datasets and three different diagnoses (**a**); 151 TMS sites across four datasets, one diagnosis (major depressive disorder) and four different TMS targets (**b**); and 101 DBS sites across five datasets, three different diagnoses and four different DBS targets (**c**). OPT-TMS, Optimizing TMS for the Treatment of Depression Study; sgACC, subgenual anterior cingulate cortex; VC/VS, ventral capsule/ventral striatum; STN, subthalamic nucleus; ANT, anterior nucleus of the thalamus.

(mean spatial $r = 0.26$, 95% CI 0.19 to 0.33, $P < 0.001$) (Fig. 4b and Supplementary Fig. 2).

To assess whether this result was driven by overall clinical severity/disability rather than depression, this analysis was repeated using the severity of the primary presenting symptom in non-MDD datasets. This control analysis included stroke severity, PD motor improvement or seizure frequency improvement. Control circuit maps from non-MDD datasets failed to match depression circuit maps from MDD datasets (mean spatial $r = -0.03$, 95% CI −0.09 to 0.03, $BF_{01} = 1.04$), and this spatial cross-correlation was significantly weaker than the cross-correlation between the depression circuit maps used in our primary analysis ($P < 0.001$) (Fig. 4b).

To assess specificity to depression versus other cognitive or emotional symptoms, we generated control circuit maps using 34 other cognitive/emotional scores, which were available in our two largest datasets (Vietnam Head Injury Study (VHIS) and St. Louis). Our leave-one-dataset-out depression circuit map (generated from the other 13 datasets) was more similar

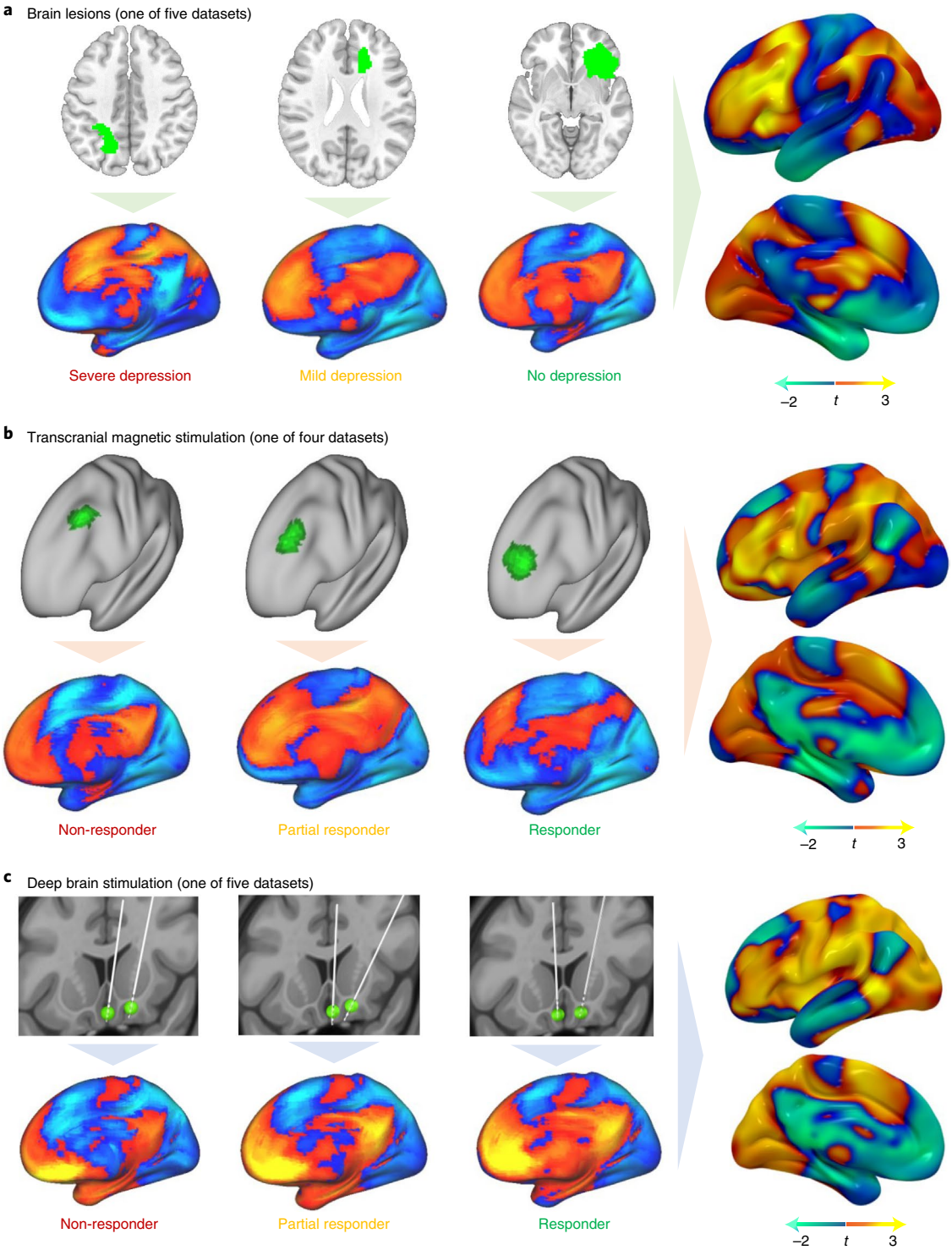

Fig. 2 | Identifying depression circuit maps for each cohort. a–c, Brain lesions (**a**), TMS sites (**b**) and DBS sites (**c**) were all mapped to a common brain atlas (top row of each panel). Functional connectivity of each lesion location or stimulation site was computed using a normative connectome database (bottom row of each panel). Positive functional connectivity is shown in warm colours (red, orange, yellow), and negative functional connectivity in cool colours (blue, teal, green). Connections most associated with depression score (lesion datasets) or change in depression score (brain stimulation datasets) were identified for each dataset (right column). The colour scale was inverted for TMS datasets because TMS sites that improve depression are thought to be anti-correlated to DBS sites that improve depression or lesion sites associated with lower risk of depression.

to the VHIS depression circuit map than to the 28 control circuit maps ($r = 0.54$ versus $r < 0.35$) (Supplementary Fig. 3a). Our leave-one-dataset-out depression circuit map was also more similar to the St. Louis depression circuit map than to the six control circuit maps ($r = 0.39$ versus $r < 0.23$) (Supplementary Fig. 3b). Across both datasets, the leave-one-dataset-out maps were significantly more similar to the depression circuit maps than to the other circuit maps ($P = 0.0032$).

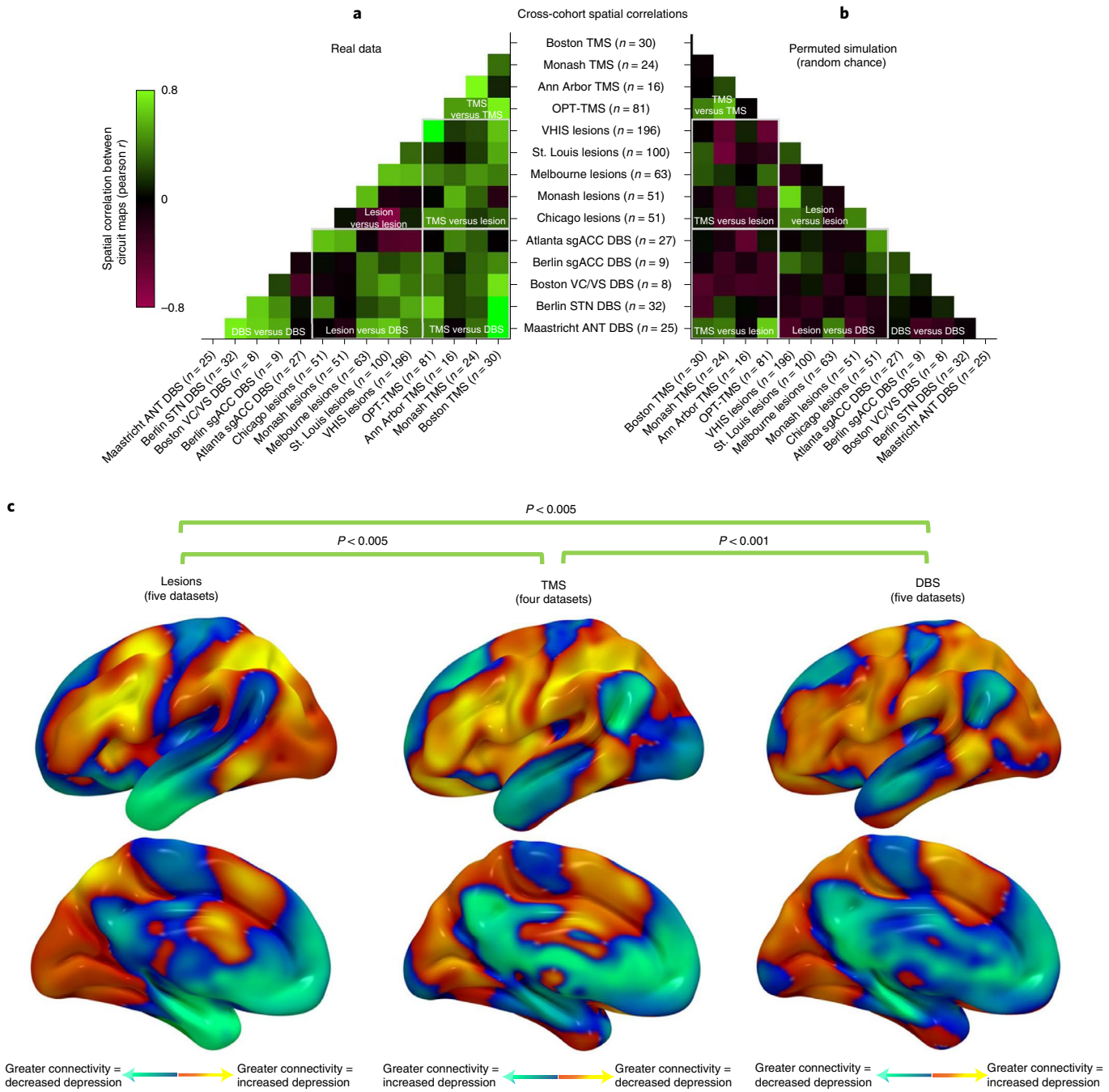

Fig. 3 | Depression circuit maps are similar across 14 datasets ($n = 713$). a, The 14 circuit maps were consistently similar to one another (mean $r = 0.24$, 95% CI 0.19 to 0.29), as depicted in this cross-correlogram comparing different datasets. Permutation testing confirmed that the weighted mean cross-correlation was significantly stronger than expected by chance ($P < 0.001$, 10,000 permutations). Green colours represent high spatial correlation between circuit maps, black boxes represent neutral correlation and red boxes represent negative correlation. **b**, Representative example of correlation between circuit maps generated from randomly permuted data. This analysis confirmed that no overall cross-correlation is expected by chance (mean $r = 0.00$, 95% CI −0.01 to 0.01). **c**, Depression circuit maps were similar between lesion datasets ($n = 461$), TMS datasets ($n = 151$) and DBS datasets ($n = 101$). Permutation testing confirmed that each comparison was significantly stronger than expected by chance ($P < 0.005$, 10,000 permutations). For display purposes, depression circuit maps were averaged (weighted mean) across datasets within each modality. The colour scale on TMS circuit maps is inverted to facilitate visual comparison with lesion and DBS circuit maps.

Combining all datasets and explaining clinical variance. We generated a combined depression circuit map by taking the mean of all 14 circuit maps, weighted by the sample size of each dataset (Fig. 5a). Peak regions in this combined map include the intraparietal sulcus, dorsolateral prefrontal cortex, inferior frontal gyrus, ventromedial prefrontal cortex and subgenual cingulate cortex (Supplementary Table 2). Compared with a consensus brain network parcellation[24], our circuit was most similar to the dorsal attention network and frontoparietal control network, and was most anti-correlated to the default mode network and limbic network (Supplementary Fig. 4).

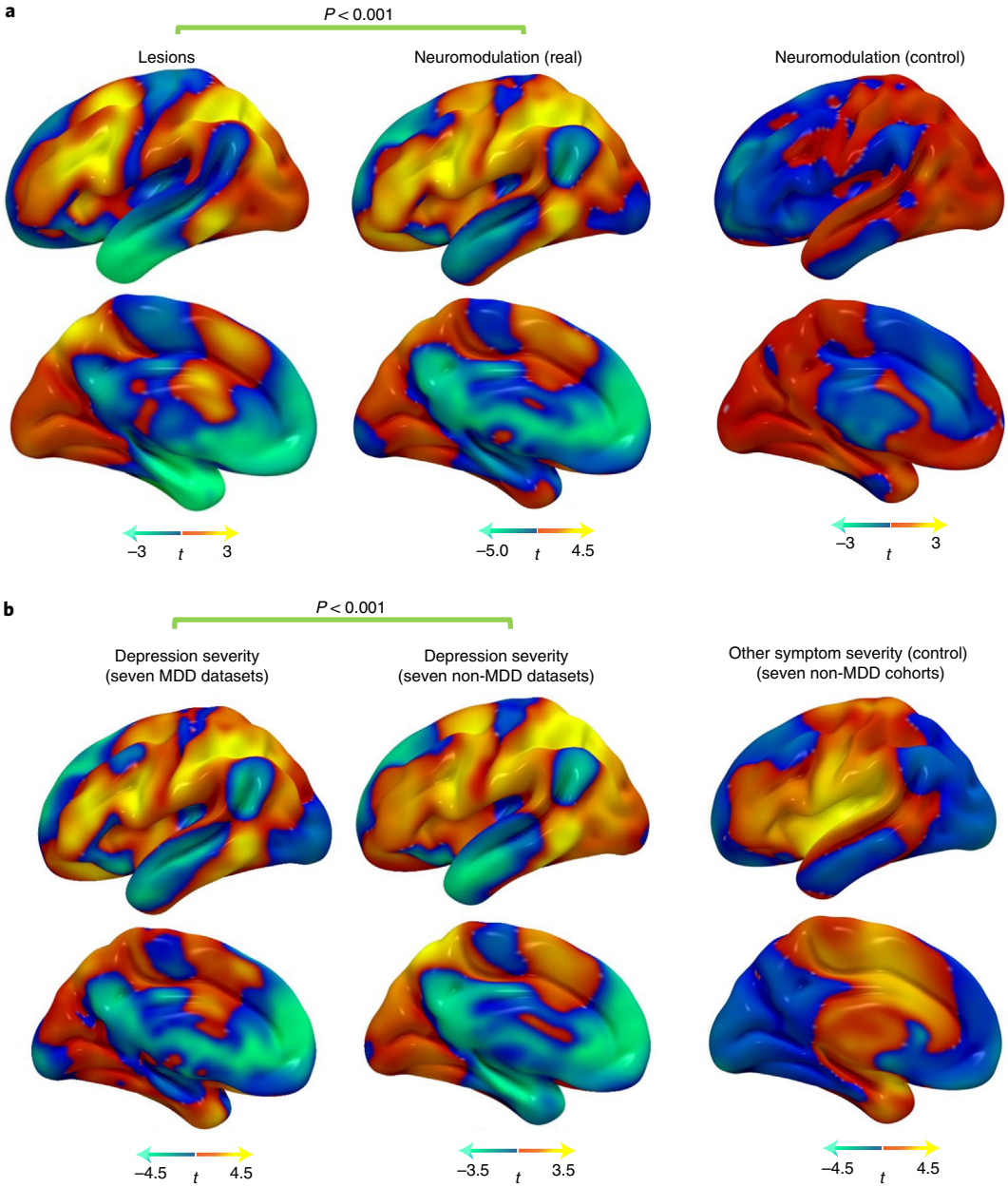

Fig. 4 | Depression circuit maps are similar across lesions, neuromodulation and diagnoses. a, Depression circuit maps were similar between lesion datasets and neuromodulation datasets (mean $r = 0.25$, 95% CI 0.16 to 0.34). Permutation testing confirmed that this similarity was stronger than expected by chance ($P < 0.001$, 10,000 permutations). In a control analysis, there was no similarity between depression circuit maps from lesion datasets and age-based circuit maps from neuromodulation datasets ($r = -0.11$, 95% CI −0.21 to −0.01, $P = 0.93$). **b**, Depression circuit maps were similar between MDD patients and non-MDD patients (mean $r = 0.26$, 95% CI 0.16 to 0.36, $P < 0.001$). Permutation testing confirmed that this similarity was stronger than expected by chance ($P < 0.001$, 10,000 permutations). In a control analysis, there was no similarity between depression circuit maps from MDD datasets and 'other symptom severity' circuit maps in non-MDD datasets ($r = -0.03$, 95% CI −0.12 to 0.06, $P = 0.77$).

In a leave-one-dataset-out analysis, we assessed whether connectivity of the stimulation site to our depression circuit could predict depression outcomes after TMS and DBS. In each neuromodulation dataset, each patient's stimulation site connectivity profile was compared with a circuit map generated from the remaining 13 datasets using spatial correlations. Across all neuromodulation datasets, connectivity to our circuit predicted the efficacy of treatment targets (weighted mean $r = 0.22$, 95% CI 0.11 to 0.33 $P < 0.001$) (Fig. 5b). The leave-one-dataset-out circuit independently predicted clinical variance in TMS datasets (weighted mean $r = 0.24$, $P = 0.0034$) and DBS datasets (weighted mean $r = 0.21$, $P = 0.033$).

Comparison with prior established methods. We hypothesized that our mapping and targeting approach would outperform established methods for both causal brain mapping and neuromodulation targeting. First, we repeated the primary analysis using voxel-lesion symptom mapping (VLSM), a tool that is widely used to localize behaviours using lesions[25]. Similar approaches have also been applied to TMS[16] and DBS[26]. VLSM failed to detect significant similarity across all 14 datasets (mean spatial $r = -0.03$, $P = 0.91$, $BF_{01} = 1.001$).

Next, we compared our approach with existing approaches for connectivity-based neuromodulation targeting. For each TMS

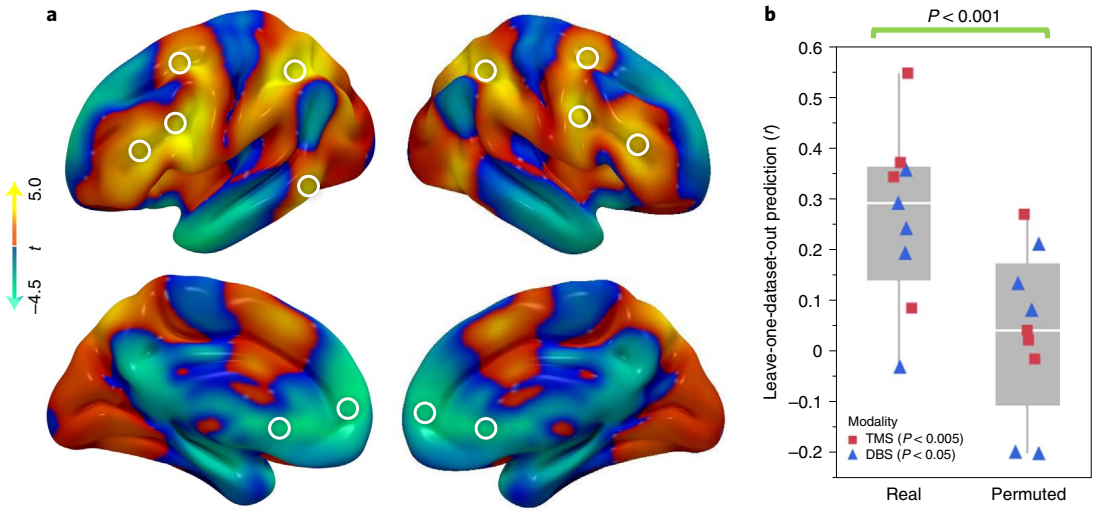

Fig. 5 | Combining all circuit maps and predicting clinical variance. a, A combined 'depression circuit' was generated from all 14 datasets. Peaks in this circuit are depicted by white circles. Positive peaks included the dorsolateral prefrontal cortex, frontal eye fields, inferior frontal gyrus, intraparietal sulcus and extrastriate visual cortex. Negative peaks included the subgenual cingulate cortex and ventromedial prefrontal cortex. Peaks are listed in Supplementary Table 2. **b**, Across the 9 neuromodulation cohorts ($n=252$), antidepressant efficacy was predicted by stimulation site connectivity to a circuit generated from the remaining 13 cohorts (mean $r=0.22$), shown as the median (line), interquartile range (box limits), outliers (whiskers) and the individual correlation value for each neuromodulation (points). Permutation testing confirmed that this similarity was stronger than expected by chance ($P<0.001$, 10,000 permutations). This was true for both TMS ($n=151$, $r=0.24$, $P=0.0034$ with 10,000 permutations) and DBS ($n=101$, $r=0.21$, $P=0.033$ with 10,000 permutations).

and DBS site, we computed connectivity to the subgenual cingulate cortex, which has been shown to predict TMS response[8,18] and has been used as a DBS target[27]. Indeed, antidepressant efficacy of each stimulation site was correlated with its connectivity to the subgenual cingulate (weighted mean $r=-0.13$, 95% CI −0.24 to −0.02, $P=0.039$). Connectivity to our leave-one-dataset-out depression circuit predicted outcomes (weighted mean $r=0.22$, 95% CI 0.11 to 0.33, $P<0.001$) significantly better than connectivity to the subgenual cingulate ($P=0.012$).

Generalizability of the method beyond depression. To demonstrate that this approach can generalize to other neuropsychiatric disorders, we also repeated the analysis using previously published data on motor symptoms of PD, the most common clinical indication for DBS. This included 29 case reports of lesion-induced parkinsonism[28], 95 patients (two datasets) who received DBS for PD[28] and one TMS site (primary motor cortex, hand knob) which demonstrated efficacy for PD in a meta-analysis of ten randomized trials[29].

The PD circuit derived from lesions was similar to the PD circuit derived from DBS ($P=0.01$) (Supplementary Fig. 5). Connectivity to the motor cortex TMS target predicted change in PD motor symptoms with DBS ($P=0.02$) and risk of parkinsonism after a brain lesion ($P=0.0005$) (Supplementary Fig. 5). In a leave-one-dataset-out analysis, the PD circuit predicted motor improvement with DBS ($r=0.26$, $P=0.01$).

To confirm specificity, we used the PD circuit as a control for depression and vice versa. Connectivity to the PD circuit was independently predictive of motor improvement ($P=0.0003$) after controlling for connectivity to the depression circuit. Connectivity to the depression circuit was independently predictive of mood improvement ($P=0.02$) after controlling for connectivity to the PD circuit. By itself, the depression circuit did not significantly predict motor improvement with DBS ($r=-0.06$, $P=0.58$, $BF_{01}=3.4$). The PD circuit also did not significantly predict depression improvement with TMS and DBS ($r=0.06$, $P=0.32$), although Bayesian analysis indicates moderate evidence for a correlation ($BF_{01}=0.29$).

Discussion

Across 14 independent datasets, we found that mapping depression based on brain lesions, TMS sites and DBS sites converged on a common neuroanatomical substrate. This convergence was robust despite many sources of heterogeneity that should bias us against a common substrate, including different lesion distributions, lesion aetiologies, stimulation targets, stimulation modalities and neuropsychiatric diagnoses. Our convergent circuit includes regions previously implicated in depression such as the subgenual cingulate, ventromedial prefrontal cortex and dorsolateral prefrontal cortex[30–34]. However, our different datasets converged on a common brain circuit or brain network, not an individual brain region. The circuit was consistent with prior work on large-scale brain networks in depression, as it is similar to the dorsal attention network and the frontoparietal control network and anti-correlated with the default mode network and limbic network[35]. This neuroanatomical convergence has several important implications.

First, TMS sites and DBS sites that modulate depression were connected to a similar circuit. To our knowledge, this is the strongest evidence to date that invasive and non-invasive brain stimulation are targeting the same circuit to treat the same symptom[12,13]. Given recent negative trials of DBS[20,36] and TMS[37] for depression, our circuit may serve as a refined therapeutic target to improve neuromodulation outcomes in future trials. More broadly, this finding supports the use of circuit mapping to define neuromodulation targets[6,8,9] and translate therapy between stimulation modalities for various neuropsychiatric disorders[13]. Furthermore, our findings support the notion that high-frequency TMS and high-frequency DBS modulate brain circuits in opposite directions[13], as the TMS and DBS maps were inverted with respect to each other.

Second, lesion locations associated with depression and stimulation sites that modulate depression were connected to a similar circuit. This finding generalized to Parkinson's disease as lesion locations associated with parkinsonism and stimulation sites that modulate parkinsonism were connected to a similar circuit, which was distinct from our depression circuit. To our knowledge, this is the strongest evidence to date showing that lesions causing a

symptom can identify therapeutic targets for symptom relief. Given that lesion network mapping has been used to map a broad range of neuropsychiatric symptoms, from amnesia to criminality[5], our approach may have therapeutic implications well beyond depression and Parkinson's disease.

Third, we identified similar depression circuits in patients with MDD, penetrating brain injury, stroke, epilepsy and PD. This suggests that depression symptoms map to a similar neuroanatomical substrate independent of whether the symptoms are caused by a primary psychiatric disorder, a structural brain lesion or a side effect of DBS. This finding is consistent with the recent Research Domain Criteria initiative, which seeks to establish transdiagnostic constructs for psychiatric symptom severity[38]. Our findings were also specific to depression relative to other neuropsychiatric symptoms, but further work is needed to conclusively confirm specificity.

Fourth, our findings were consistent across 14 independent datasets. Most prior studies in depression have focused on a single dataset[30–34], although larger studies are beginning to appear[14]. Meta-analyses often find poor consistency in neuroimaging correlates of depression[33,34]. To our knowledge, our consistency across 14 datasets, including a leave-one-dataset-out analysis, is one of the strongest demonstrations of result consistency for a psychiatric condition. Furthermore, the results survived rigorous permutation-based statistical testing, a highly conservative approach that prevents type I error due to multiple comparisons or a biased analysis.

Fifth, it is worth highlighting our focus on 'causal' sources of information such as lesions and brain stimulation. This resolves some of the interpretive ambiguity associated with neuroimaging correlates of depressive symptoms or antidepressant efficacy of non-anatomically targeted treatments[39]. By combining brain lesions and brain stimulation, this study moves us towards the goal of "mapping causal circuitry in human depression"[2], potentially facilitating more direct translation to targeted therapeutics.

Finally, our parsimonious mapping and targeting model outperformed established approaches for both lesion-based brain mapping and connectivity-based neuromodulation targeting. Our approach identified relationships that were not apparent using VLSM, illustrating the potential of brain connectivity to detect trends beyond what is possible using anatomical location alone. Our approach also explained more clinical variance than subgenual connectivity, which is widely used to target neuromodulation[40–44].

Our analysis may seem circular or biased given that the TMS and DBS sites for MDD were chosen because they were already known to be part of a 'depression circuit'. However, our depression circuit was derived from the variance across stimulation sites within each target, not simply the location of the intended target. For example, the left prefrontal cortex appears as part of our depression circuit not because it was targeted with TMS but because different TMS sites across the left prefrontal cortex produced different effects on depression, different DBS sites produced different effects on depression symptoms depending on their connectivity to the left prefrontal cortex and different lesion locations were associated with different amounts of depression depending on their connectivity to left prefrontal cortex. It is also worth noting that this concern is not relevant for lesions, which were randomly distributed throughout the brain yet identified a depression circuit that was very similar to the circuit identified from TMS or DBS sites.

There are several limitations. First, this analysis was retrospective, taking advantage of existing datasets with heterogeneous populations and outcome metrics, limiting the amount of variance that can be explained. Prospective validation is required to confirm whether targeting our circuit results in improved antidepressant response. Second, most datasets only included a single depression score without subscales, which may also limit the amount of variance that can be explained. Given that different symptom clusters respond to stimulation of different circuits with TMS[6], future work with more detailed phenotyping may enable further subclassification. Third, we used a normative functional connectome for all circuit mapping, as prior work suggests that using a disease-matched connectome makes little difference for either depression or Parkinson's disease[6,8]. However, this analysis could be repeated using connectomes that are age, gender and disease matched to each dataset. Similarly, this analysis could be repeated using measures of structural white matter connectivity or individualized functional connectivity[9,18,45]. Individualized connectivity may explain additional variance, but adds additional noise to the analysis[46]. Individualized neurostimulation-induced electric field modelling may also be valuable, but prior work has shown it to yield similar functional connectivity estimates to our simplified model[47].

In conclusion, these results support the existence of at least one neuroanatomical substrate for depression symptoms. More broadly, by combining lesion locations, non-invasive stimulation sites and invasive stimulation sites, we introduce a method for identifying a convergent neuroanatomical substrate for neurological and psychiatric symptoms. Future work should seek to prospectively determine whether this convergent substrate provides an improved target for neuromodulation therapies.

Methods

Characteristics of included datasets. We sought out multiple datasets that included magnetic resonance imaging or computed tomography of focal brain lesions and stimulation sites. Lesions and stimulation sites showed incidentally variable locations in different patients. Localization methods are described in the Supplementary Information. All depression datasets included continuous scores on a validated depression metric. All PD datasets included either a clear case description of lesion-induced parkinsonism or continuous scores on the Unified Parkinson's Disease Rating Scale (UPDRS). In each dataset, participants provided informed consent to data collection or the institutional review board approved retrospective analysis of symptom and imaging data.

Patients with missing data were excluded from the analysis. To avoid bias due to unequal variances, unequal sample sizes or inconsistent severity cut-offs for different datasets, each dataset was analysed independently. Study characteristics are summarized in Supplementary Table 1.

No statistical methods were used to pre-determine sample size, but our sample sizes are larger than the largest prior studies of lesions[7], TMS sites[6] or DBS sites[21] in depression.

Generation of circuit maps. A normative human connectome database was used to compute mean resting-state functional connectivity of each patient's lesion or stimulation site based on 1,000 healthy subjects, as previously described[5–7]. This yielded a whole-brain connectivity map of each patient's lesion or stimulation site (Fig. 2).

In the TMS and DBS datasets with depression outcomes, these connectivity maps were compared with change in depression score using partial Pearson correlation at each voxel, controlling for pre-treatment depression severity. In the lesion datasets with depression outcomes, connectivity maps were compared with overall depression scores using Pearson correlation at each voxel. For each dataset, this analysis yielded a whole-brain 'circuit map' of connections correlated with antidepressant efficacy (for TMS and DBS) or depression severity (for lesions). TMS-based circuit maps were multiplied by −1 because TMS sites that improve depression are thought to be anti-correlated to DBS sites that improve depression[13] or lesion sites associated with lower risk of depression[5,7]. Inverting the circuit maps for TMS also facilitates visual comparison across all three modalities (Fig. 2).

In the PD DBS datasets, patient-specific connectivity maps were compared with change in UPDRS score. The connectivity of lesions causing parkinsonism was estimated using a one-sample *t* test at each voxel. For each dataset, this yielded a whole-brain circuit map of connections associated with parkinsonism. In the absence of individualized TMS sites, we generated a group-mean region of interest at the M1 hand knob (MNI coordinates [−40, −20, 62]), which has been shown to be the most effective TMS target for Parkinson's disease[29].

We generated control circuit maps using two different approaches. For all datasets, control maps were generated using patient age, which is presumably unrelated to stimulation site or lesion location, rather than depression scores. For all non-MDD datasets, additional control maps were generated using severity of the primary presenting symptom, including National Institutes of Health Stroke Scale (stroke patients), Neurobehavioral Rating Scale (penetrating brain injury patients), UPDRS (Parkinson's disease patients) and seizure frequency (epilepsy patients).

Computational and statistical methods. All computational/statistical analyses were conducted using customized MATLAB scripts, except as otherwise specified.

All correlation coefficients were Fisher-transformed before further analysis. To facilitate comparison across datasets with different sample sizes, voxel-wise Fisher z values were converted to t values. All parametric P values were computed using a two-tailed hypothesis test. Similarity between different maps was assessed using spatial correlations.

To confirm similarity across different datasets, we computed the mean spatial cross-correlation between the circuit maps in each analysis. Because the datasets were collected in highly heterogeneous settings, they could not be assumed to have identical distributions. To address this, statistical significance was addressed using a non-parametric multi-level block permutation testing approach. In this permutation test, the mean spatial correlation was re-computed 25,000 times in simulated data. The null distribution of this permutation test was defined by randomly re-assigning each patient's connectivity map with a different patient's clinical variables within the same dataset. A P value was defined as the percentage of randomly permuted results that were stronger than the real result, as in prior work[6].

For null findings, the resulting t values were used to compute BFs, which were used to compare likelihood of the null hypothesis with the likelihood of the alternative hypothesis[48]. In the case of spatial correlations, the null hypothesis was that there is no similarity between the two maps in question. Thus, for the purpose of calculating BFs, stronger positive correlations were considered to support the alternative hypothesis, while weaker positive correlations and negative correlations were considered to support the null hypothesis[49].

Combining and comparing circuit maps. The 14 circuit maps were then categorized to assess for similarity between different modalities or diagnoses. Categories included TMS, DBS, neuromodulation (TMS and DBS combined), lesions, MDD (all modalities) and non-MDD (all modalities). MDD and non-MDD datasets were defined according to the inclusion criteria of the original study. We hypothesized that (1) TMS, DBS and lesion datasets would yield similar circuits, (2) lesions and neuromodulation would yield similar circuits and (3) MDD and non-MDD patients would yield similar circuits. To statistically compare different categories, we computed the mean spatial cross-correlation of all circuit maps in one category with all circuit maps in the other category. Significance was assessed using permutation testing as above.

To visualize the map for each category, circuit maps from different datasets were combined into a mean circuit map across all voxels, weighted by the sample size of each dataset. This weighted mean approach was chosen over a combined linear model because it maintains independence between datasets, thus reducing the statistical penalty associated with combining heterogeneous datasets[50].

Each dataset's circuit map was also compared with a leave-one-dataset-out circuit map generated by taking the weighted mean of the other 13 circuit maps. This yielded a leave-one-dataset-out spatial correlation for each dataset. The weighted mean of these spatial correlations was considered to represent the overall similarity between each circuit map and the remaining circuit maps. This value was assessed for significance using permutation testing as above.

Assessing specificity to depression. To confirm that the results were not driven by overall clinical severity, we repeated the analysis using the control circuit maps generated from severity of non-depressive symptoms in non-MDD datasets. Using the same statistical methods described above, we hypothesized that (1) the control circuit maps would not be significantly similar between different datasets, modalities or diagnoses and (2) the control circuit maps would not significantly match the depression circuit maps. We also hypothesized that the spatial cross-correlation between depression circuit maps would be significantly stronger than the spatial cross-correlation between control circuit maps using a paired t test.

To assess specificity to depression, we then generated symptom-specific circuit maps based on other cognitive/emotional scales, which were available in our two largest datasets. In the VHIS dataset ($n=196$), we generated 28 circuit maps based on the Mini Mental State Examination and each of the 27 symptoms measured by the Neurobehavioral Rating Scale. In the St. Louis dataset ($n=100$), we generated six circuit maps based on the Boston Naming Test, animal naming test (verbal fluency), Hopkins Verbal Learning Test (learning/memory), Brief Visuospatial Memory Test (visual memory), clock draw test (visuospatial skills) and spatial span test (attention). In each dataset, we used spatial correlations to compare the symptom-specific maps with a leave-one-dataset-out depression map generated from the other 13 datasets. We hypothesized that the leave-one-dataset-out depression maps would be more similar to each dataset's depression map than to its other symptom-specific maps.

To test for significance, we regenerated these cognitive/emotional circuit maps 25,000 times after randomly permuting each patient's clinical outcomes with a different patient's neuroimaging results. We again used spatial correlation to compare each of these maps with a leave-one-dataset-out depression map. We averaged the resulting Fisher-transformed spatial correlations, yielding a null distribution of 25,000 spatial correlation values expected by random chance. We computed a P value as the percentage of these values that exceeded the weighted mean correlation between the leave-one-dataset-out map and each dataset's depression circuit map.

Explaining clinical variance. For each neuromodulation dataset, treatment-induced change in depression score was predicted using a leave-one-dataset-out map constructed from the other 13 datasets. Within each dataset, spatial correlations were computed between each patient's stimulation site connectivity profile and the leave-one-dataset-out map. This yielded a metric representing the similarity between the patient's stimulation site connectivity and the 'ideal' stimulation site connectivity. In each dataset, this similarity metric was compared with improvement in depression score using partial Pearson correlation, controlling for baseline depression severity. Across all datasets, these correlations were combined into a single weighted mean value representing the degree to which our circuit predicted neuromodulation outcomes across all datasets. Significance was assessed using permutation testing as above.

Finally, a combined depression circuit map was generated based on the weighted mean of all 14 datasets. Peaks in this circuit map were identified using the functional MRI (fMRI) of the brain software library (FSL) 'cluster' algorithm with a detection threshold of $P<0.00005$ and minimum cluster extent of 100 mm^3, consistent with conservative statistical guidelines[51].

Comparison with prior established methods. We hypothesized that our model would be superior to existing methods for both causal brain mapping and neuromodulation targeting. First, we compared our causal mapping approach with VLSM, a tool that can identify lesion locations or stimulation sites associated with a particular behavioural outcome (without considering connectivity)[25]. Next, we compared our connectivity-based targeting approach with the current consensus approach, which identifies optimal TMS targets based on subgenual cingulate connectivity[8,18].

Using VLSM, we assessed whether particular lesion locations and stimulation sites were associated with depression, irrespective of their connectivity. At each voxel, we used a t test to compare depression severity between patients whose lesions or stimulation sites overlapped with that voxel versus patients whose lesions or stimulation sites did not overlap with that voxel. This yielded a whole-brain map of lesion locations or stimulation sites associated with depression severity.

We then attempted to explain clinical variance using stimulation site connectivity to the subgenual cingulate. Within each dataset, we computed the mean connectivity of each patient's stimulation site to the subgenual cingulate, following the methods described in ref. [8]. In each dataset, subgenual connectivity was compared with improvement in depression score using partial Pearson correlation, controlling for baseline depression severity. Across all datasets, these correlations were combined into a single weighted mean value representing the degree to which our circuit predicted neuromodulation outcomes across all datasets. The predictive value of subgenual connectivity was compared with the predictive value of our depression circuit using a Z test for dependent correlations within each dataset.

Reporting summary. Further information on research design is available in the Nature Research Reporting Summary linked to this article.

Data availability statement

This paper used de-identified data from 14 different datasets collected by 14 different teams of investigators at various institutions across four different countries. Each dataset is available upon reasonable request from each respective team of investigators. Data sharing will be subject to the policies and procedures of the institution where each dataset was collected as well as the laws of the country where each dataset was collected.

Code availability statement

All custom MATLAB code used in this study is available upon reasonable request from the corresponding author.

Received: 30 December 2020; Accepted: 11 June 2021;
Published online: 08 July 2021

References

1. Czéh, B., Fuchs, E., Wiborg, O. & Simon, M. Animal models of major depression and their clinical implications. *Prog. Neuro-Psychopharmacol. Biol. Psychiatry* **64**, 293–310 (2016).
2. Etkin, A. Mapping causal circuitry in human depression. *Biol. Psychiatry* **86**, 732–733 (2019).
3. Nestler, E. J. & Hyman, S. E. Animal models of neuropsychiatric disorders. *Nat. Neurosci.* **13**, 1161–1169 (2010).
4. Monteggia, L. M., Heimer, H. & Nestler, E. J. Meeting report: can we make animal models of human mental illness? *Biol. Psychiatry* **84**, 542–545 (2018).
5. Fox, M. D. Mapping symptoms to brain networks with the human connectome. *N. Engl. J. Med* **379**, 2237–2245 (2018).
6. Siddiqi, S. H. et al. Distinct symptom-specific treatment targets for circuit-based neuromodulation. *Am. J. Psychiatry* **177**, 435–446 (2020).
7. Padmanabhan, J. L. et al. A human depression circuit derived from focal brain lesions. *Biol. Psychiatry* https://doi.org/10.1016/j.biopsych.2019.07.023 (2019).

8. Weigand, A. et al. Prospective validation that subgenual connectivity predicts antidepressant efficacy of transcranial magnetic stimulation sites. *Biol. Psychiatry* **84**, 28–37 (2018).
9. Riva-Posse, P. et al. Defining critical white matter pathways mediating successful subcallosal cingulate deep brain stimulation for treatment-resistant depression. *Biol. Psychiatry* **76**, 963–969 (2014).
10. Etkin, A. Addressing the causality gap in human psychiatric neuroscience. *JAMA Psychiatry* **75**, 3–4 (2018).
11. Ressler, K. J. & Mayberg, H. S. Targeting abnormal neural circuits in mood and anxiety disorders: from the laboratory to the clinic. *Nat. Neurosci.* **10**, 1116–1124 (2007).
12. Matthews, P. M. & Hampshire, A. Clinical concepts emerging from fMRI functional connectomics. *Neuron* **91**, 511–528 (2016).
13. Fox, M. D. et al. Resting-state networks link invasive and noninvasive brain stimulation across diverse psychiatric and neurological diseases. *Proc. Natl Acad. Sci. USA* **111**, E4367–E4375 (2014).
14. Drysdale, A. T. *et al.* Resting-state connectivity biomarkers define neurophysiological subtypes of depression. *Nat. Med.* https://doi.org/10.1038/nm.4246 (2016).
15. Koenigs, M. et al. Focal brain damage protects against post-traumatic stress disorder in combat veterans. *Nat. Neurosci.* **11**, 232–237, https://doi.org/10.1038/nn2032 (2008).
16. Johnson, K. A. et al. Prefrontal rTMS for treating depression: location and intensity results from the OPT-TMS multi-site clinical trial. *Brain Stimul.* **6**, 108–117 (2013).
17. Taylor, S. F. et al. Changes in brain connectivity during a sham-controlled, transcranial magnetic stimulation trial for depression. *J. Affect Disord.* **232**, 143–151 (2018).
18. Cash, R. F. H. et al. Subgenual functional connectivity predicts antidepressant treatment response to transcranial magnetic stimulation: independent validation and evaluation of personalization. *Biol. Psychiatry* **86**, e5–e7 (2019).
19. Horn, A. et al. Connectivity predicts deep brain stimulation outcome in Parkinson disease. *Ann. Neurol.* **82**, 67–78 (2017).
20. Dougherty, D. D. et al. A randomized sham-controlled trial of deep brain stimulation of the ventral capsule/ventral striatum for chronic treatment-resistant depression. *Biol. Psychiatry* **78**, 240–248 (2015).
21. Irmen, F. *et al.* Left prefrontal impact links subthalamic stimulation with depressive symptoms. *Ann. Neurol.* https://doi.org/10.1002/ana.25734 (2020).
22. Merkl, A. et al. Antidepressant effects after short-term and chronic stimulation of the subgenual cingulate gyrus in treatment-resistant depression. *Exp. Neurol.* **249**, 160–168 (2013).
23. Schaper, F. L. W. V. J. et al. Deep brain stimulation in epilepsy: a role for modulation of the mammillothalamic tract in seizure control? *Neurosurgery* **87**, 602–610 (2020).
24. Yeo, B. T. et al. The organization of the human cerebral cortex estimated by intrinsic functional connectivity. *J. Neurophysiol.* **106**, 1125–1165 (2011).
25. Bates, E. et al. Voxel-based lesion–symptom mapping. *Nat. Neurosci.* **6**, 448–450 (2003).
26. Gourisankar, A. et al. Mapping movement, mood, motivation and mentation in the subthalamic nucleus. *R. Soc. Open Sci.* **5**, 171177 (2018).
27. Choi, K. S., Riva-Posse, P., Gross, R. E. & Mayberg, H. S. Mapping the "depression switch" during intraoperative testing of subcallosal cingulate deep brain stimulation. *JAMA Neurol.* **72**, 1252–1260 (2015).
28. Joutsa, J., Horn, A., Hsu, J. & Fox, M. D. Localizing parkinsonism based on focal brain lesions. *Brain* **141**, 2445–2456 (2018).
29. Yang, C. et al. Repetitive transcranial magnetic stimulation therapy for motor recovery in Parkinson's disease: a meta-analysis. *Brain Behav.* **8**, e01132 (2018).
30. James, G. A. et al. Exploratory structural equation modeling of resting-state fMRI: applicability of group models to individual subjects. *NeuroImage* **45**, 778–787 (2009).
31. Mayberg, H. S. et al. Reciprocal limbic-cortical function and negative mood: converging PET findings in depression and normal sadness. *Am. J. Psychiatry* **156**, 675–682 (1999).
32. Drevets, W. C. et al. Subgenual prefrontal cortex abnormalities in mood disorders. *Nature* **386**, 824–827 (1997).
33. Müller, V. I. et al. Altered brain activity in unipolar depression revisited: meta-analyses of neuroimaging studies. *JAMA Psychiatry* **74**, 47–55 (2017).
34. Gray, J. P., Müller, V. I., Eickhoff, S. B. & Fox, P. T. Multimodal abnormalities of brain structure and function in major depressive disorder: a meta-analysis of neuroimaging studies. *Am. J. Psychiatry* **177**, 422–434 (2020).
35. Williams, L. M. Defining biotypes for depression and anxiety based on large-scale circuit dysfunction: a theoretical review of the evidence and future directions for clinical translation. *Depress. Anxiety* **34**, 9–24 (2017).
36. Holtzheimer, P. E. et al. Subcallosal cingulate deep brain stimulation for treatment-resistant depression: a multisite, randomised, sham-controlled trial. *Lancet Psychiatry* **4**, 839–849 (2017).
37. Yesavage, J. A. et al. Effect of repetitive transcranial magnetic stimulation on treatment-resistant major depression in US veterans: a randomized clinical trial. *JAMA Psychiatry* **75**, 884–893 (2018).
38. Kozak, M. J. & Cuthbert, B. N. The NIMH Research Domain Criteria initiative: background, issues, and pragmatics. *Psychophysiology* **53**, 286–297 (2016).
39. Poldrack, R. A. Inferring mental states from neuroimaging data: from reverse inference to large-scale decoding. *Neuron* **72**, 692–697 (2011).
40. Cole, EleanorJ. et al. Stanford accelerated intelligent neuromodulation therapy for treatment-resistant depression. *Am. J. Psychiatry* https://doi.org/10.1176/appi.ajp.2019.19070720 (2020).
41. Blumberger, D. M. et al. Effectiveness of theta burst versus high-frequency repetitive transcranial magnetic stimulation in patients with depression (THREE-D): a randomised non-inferiority trial. *Lancet* **391**, 1683–1692 (2018).
42. Cash, R. F. H. *et al.* Using brain imaging to improve spatial targeting of transcranial magnetic stimulation for depression. *Biol. Psychiatry* https://doi.org/10.1016/j.biopsych.2020.05.033 (2020).
43. Cash, R. F. H., Cocchi, L., Lv, J., Fitzgerald, P. B. & Zalesky, A. Functional magnetic resonance imaging-guided personalization of transcranial magnetic stimulation treatment for depression. *JAMA Psychiatry*, https://doi.org/10.1001/jamapsychiatry.2020.3794 (2020).
44. Siddiqi, S. H., Weigand, A., Pascual-Leone, A. & Fox, M. D. Identification of personalized TMS targets based on subgenual cingulate connectivity: an independent replication. *Biol. Psychiatry* https://doi.org/10.1016/j.biopsych.2021.02.015 (2021).
45. Riva-Posse, P. et al. A connectomic approach for subcallosal cingulate deep brain stimulation surgery: prospective targeting in treatment-resistant depression. *Mol. Psychiatry* **23**, 843–849 (2018).
46. Fox, M. D., Liu, H. & Pascual-Leone, A. Identification of reproducible individualized targets for treatment of depression with TMS based on intrinsic connectivity. *Neuroimage* **66**, 151–160 (2013).
47. Opitz, A., Fox, M. D., Craddock, R. C., Colcombe, S. & Milham, M. P. An integrated framework for targeting functional networks via transcranial magnetic stimulation. *Neuroimage* **127**, 86–96 (2016).
48. Rouder, J. N. & Morey, R. D. Default Bayes factors for model selection in regression. *Multivar. Behav. Res.* **47**, 877–903 (2012).
49. Wagenmakers, E.-J., Verhagen, J. & Ly, A. How to quantify the evidence for the absence of a correlation. *Behav. Res. Methods* **48**, 413–426 (2016).
50. Turner, J. A. et al. A multi-site resting state fMRI study on the amplitude of low frequency fluctuations in schizophrenia. *Front Neurosci.* **7**, 137 (2013).
51. Slotnick, S. D. Cluster success: fMRI inferences for spatial extent have acceptable false-positive rates. *Cogn. Neurosci.* **8**, 150–155 (2017).

Acknowledgements

The authors thank all research participants, funding bodies, allied health staff and other research staff that made this work possible. The present work was supported by the Sidney R. Baer Foundation (S.H.S., J.L.P., M.D.F.), the Brain & Behavior Research Foundation (SHS) and the National Institute of Mental Health (grant no. K23MH121657 to S.H.S.; grant nos. R01MH113929 and R01MH115949 to M.D.F.). The funders were not directly involved in the conceptualization, design, data collection, analysis, decision to publish or preparation of the manuscript.

Author contributions

Conception and design of study: S.H.S., A.H. and M.D.F. Design of analytical procedures: S.H.S. and M.D.F. Neuroimaging analyses and statistical analyses: S.H.S. Preprocessing and preparation of data for analysis: S.H.S., A.H., J.H., J.L.P. and F.S. Contribution of data: A.H., F.S., R.F.H.C., A.B., K.A.J., N.E., A.M.N., S.G., T.G.P., K.S.C., F.I., A.K., P.B.F., M.S.G., R.P.W.R., S.F.T., A.Z., J.L.V., M.C., D.D.D., A.P.-L., J.H.G., H.S.M. and M.D.F. Writing of manuscript: S.H.S. and M.D.F. with input from all authors.

Competing interests

S.H.S. serves as a clinical consultant for Kaizen Brain Center. S.H.S. and M.D.F. have jointly received investigator-initiated research support from Neuronetics. None of these organizations were involved in the present work. S.H.S. and M.D.F. each own independent intellectual property on the use of brain network mapping to target neuromodulation. The present work did not utilize any of this intellectual property. The authors report no other conflicts of interest related to the present work.

Additional information

Supplementary information The online version contains supplementary material available at https://doi.org/10.1038/s41562-021-01161-1.

Correspondence and requests for materials should be addressed to S.H.S.

Peer review information *Nature Human Behaviour* thanks Nolan Williams and the other, anonymous, reviewer(s) for their contribution to the peer review of this work.

Reprints and permissions information is available at www.nature.com/reprints.

Publisher's note Springer Nature remains neutral with regard to jurisdictional claims in published maps and institutional affiliations.

nature research

Corresponding author(s): Shan H. Siddiqi, MD

Last updated by author(s): 02/24/2021

Reporting Summary

Nature Research wishes to improve the reproducibility of the work that we publish. This form provides structure for consistency and transparency in reporting. For further information on Nature Research policies, see our Editorial Policies and the Editorial Policy Checklist.

Statistics

For all statistical analyses, confirm that the following items are present in the figure legend, table legend, main text, or Methods section.

n/a	Confirmed	
☐	☒	The exact sample size (*n*) for each experimental group/condition, given as a discrete number and unit of measurement
☐	☒	A statement on whether measurements were taken from distinct samples or whether the same sample was measured repeatedly
☐	☒	The statistical test(s) used AND whether they are one- or two-sided *Only common tests should be described solely by name; describe more complex techniques in the Methods section.*
☐	☒	A description of all covariates tested
☐	☒	A description of any assumptions or corrections, such as tests of normality and adjustment for multiple comparisons
☐	☒	A full description of the statistical parameters including central tendency (e.g. means) or other basic estimates (e.g. regression coefficient) AND variation (e.g. standard deviation) or associated estimates of uncertainty (e.g. confidence intervals)
☐	☒	For null hypothesis testing, the test statistic (e.g. *F*, *t*, *r*) with confidence intervals, effect sizes, degrees of freedom and *P* value noted *Give P values as exact values whenever suitable.*
☒	☐	For Bayesian analysis, information on the choice of priors and Markov chain Monte Carlo settings
☒	☐	For hierarchical and complex designs, identification of the appropriate level for tests and full reporting of outcomes
☐	☒	Estimates of effect sizes (e.g. Cohen's *d*, Pearson's *r*), indicating how they were calculated

Our web collection on statistics for biologists contains articles on many of the points above.

Software and code

Policy information about availability of computer code

Data collection	Lesion network maps was constructed using in-house scripts in combination with public human connectome data, as described in our prior work (MD Fox, NEJM 2018).
Data analysis	Except as specified otherwise, all statistical analyses were conducted using novel MATLAB scripts as described in the manuscript.

For manuscripts utilizing custom algorithms or software that are central to the research but not yet described in published literature, software must be made available to editors and reviewers. We strongly encourage code deposition in a community repository (e.g. GitHub). See the Nature Research guidelines for submitting code & software for further information.

Data

Policy information about availability of data

All manuscripts must include a data availability statement. This statement should provide the following information, where applicable:

- Accession codes, unique identifiers, or web links for publicly available datasets
- A list of figures that have associated raw data
- A description of any restrictions on data availability

This manuscript involved 14 different datasets from different institutions. Each dataset is available upon reasonable request from the investigators that collected it.

Field-specific reporting

Please select the one below that is the best fit for your research. If you are not sure, read the appropriate sections before making your selection.

☒ Life sciences ☐ Behavioural & social sciences ☐ Ecological, evolutionary & environmental sciences

For a reference copy of the document with all sections, see nature.com/documents/nr-reporting-summary-flat.pdf

Life sciences study design

All studies must disclose on these points even when the disclosure is negative.

Sample size	Because there is no standard method for estimating sample size for this type of study, we attempted to identify as many datasets as possible that linked lesions and neurostimulation sites to depression scores (or Parkinson's disease motor scores, in the case of our secondary analysis). To our knowledge, this is the largest study of its kind.
Data exclusions	All subjects with complete neuroimaging and depression scores (primary analysis) or Parkinson's disease motor scores (secondary analysis - re-analysis of our prior publications) were included.
Replication	As outlined in the manuscript, we used rigorous statistical techniques to assess overall reproducibility across multiple independent datasets. All replication attempts were successful.
Randomization	Rather than prospective randomization, this study capitalized on incidental variability of lesions, TMS sites, and DBS sites (as described in the manuscript). This incidental variability was presumed to be random, making it an instrumental variable.
Blinding	Blinding was not relevant because this was a secondary analysis of existing datasets. We mitigated the risk of observer bias by testing our previously-published hypothesis (Fox et al, PNAS 2014) in multiple independent datasets.

Reporting for specific materials, systems and methods

We require information from authors about some types of materials, experimental systems and methods used in many studies. Here, indicate whether each material, system or method listed is relevant to your study. If you are not sure if a list item applies to your research, read the appropriate section before selecting a response.

Materials & experimental systems

n/a	Involved in the study
☒	☐ Antibodies
☒	☐ Eukaryotic cell lines
☒	☐ Palaeontology and archaeology
☒	☐ Animals and other organisms
☐	☒ Human research participants
☒	☐ Clinical data
☒	☐ Dual use research of concern

Methods

n/a	Involved in the study
☒	☐ ChIP-seq
☒	☐ Flow cytometry
☐	☒ MRI-based neuroimaging

Human research participants

Policy information about studies involving human research participants

Population characteristics	In the primary analysis (major depression), participants included (1) adults who had incidental brain lesions due to penetrating trauma or stroke, (2) adults who completed depression inventories before and after therapeutic TMS for major depression, or (3) adults who completed depression inventories before and after therapeutic DBS for major depression, Parkinson's disease, or epilepsy. In the secondary analysis (Parkinson's disease), participants included (1) adults who developed parkinsonism after a focal brain lesion, and (2) adults who received therapeutic DBS for Parkinson's disease.
Recruitment	We included all relevant datasets that we were able to access. Each dataset had different recruitment parameters depending on the study type. For the primary analysis, the respective study types are listed in Table S1. For the secondary analysis, the details are described in our prior publications (Horn et al., 2017; Joutsa et al., 2018)
Ethics oversight	The study was approved by the IRB at Beth Israel Deaconess Medical Center (Boston, MA) and by the individual IRBs at each individual data collection site.

Note that full information on the approval of the study protocol must also be provided in the manuscript.

Magnetic resonance imaging

Experimental design

Design type	Individualized structural MRI and/or head CT combined with normative resting-state fMRI
Design specifications	Structural MRI or CT scans were used to localize lesions and/or stimulation sites. Normative resting-state fMRI data from a large connectome database (n=1000) were used to estimate connectivity of each site.
Behavioral performance measures	Each dataset used different depression scales (delineated in Table S1).

Acquisition

Imaging type(s)	Normative resting-state fMRI (n=1000 healthy controls) and individualized structural MRI (n=365) or head CT (n=348)
Field strength	MRI data collected using 3T scanner
Sequence & imaging parameters	Normative resting-state fMRI acquisitionn parameters: repetition time (TR) = 3,000 ms, echo time (TE) = 30 ms, flip angle (FA) = 85°, 3 × 3 × 3-mm voxels, field of view (FOV) = 216, and 47 axial slices collected with interleaved acquisition and no gap between slices. Each functional run lasted 6.2 min (124 time points). One or two runs were acquired per subject (average of 1.7 runs). Each dataset used different structural imaging parameters, as described in the manuscript.
Area of acquisition	Whole brain

Diffusion MRI ☐ Used ☒ Not used

Preprocessing

Preprocessing software	FreeSurfer + in-house preprocessing scripts, as in the GSP1000 dataset (details in Yeo et al, J Neurophysiol 2011)
Normalization	Nonlinear volume-based registration as in Friston et al, 1995
Normalization template	MNI ICBM152
Noise and artifact removal	Low-pass temporal filtering, head-motion regression, global signal regression, and ventricular and white matter signal regression
Volume censoring	Motion regression

Statistical modeling & inference

Model type and settings	Lesion network mapping or stimulation site network mapping with voxel-wise partial least squares regression model (details described in manuscript).
Effect(s) tested	Lesion datasets: Correlation between lesion connectivity and depression severity Neurostimulation datasets: Partial correlation between stimulation site connectivity and post-treatment depression severity, controlling for pre-treatment depression severity.

Specify type of analysis: ☒ Whole brain ☐ ROI-based ☐ Both

Statistic type for inference (See Eklund et al. 2016)	Voxel-wise
Correction	Whole-brain spatial correlations with permutation testing - there were no multiple comparisons because the spatial correlation yields only a single value, which was the primary metric.

Models & analysis

n/a	Involved in the study
☐	☒ Functional and/or effective connectivity
☒	☐ Graph analysis
☒	☐ Multivariate modeling or predictive analysis

Functional and/or effective connectivity	Mean Pearson correlation across the normative dataset (n=1000) for each lesion or stimulation site.